Analyst

ROYAL SOCIETY OF CHEMISTRY

PAPER

Cite this: *Analyst*, 2021, **146**, 2550

Location of carbon–carbon double bonds in unsaturated lipids using microdroplet mass spectrometry†

Kai Luo,[a] Hao Chen [b] and Richard N. Zare *[a]

Received 15th December 2020,
Accepted 8th March 2021

DOI: 10.1039/d0an02396e

rsc.li/analyst

An aqueous solution containing unsaturated fatty acids (100 μM) or lipids (50 μg mL^{-1}) and chloroauric acid ($HAuCl_4$, 10 μM) is electrosprayed (−4.5 kV for unsaturated fatty acids and +4.0 kV for lipids) from a 50 μm diameter capillary with N_2 nebulizing gas (60 psi), and the resulting microdroplets enter a mass spectrometer with a flight distance of 10 mm for chemical analysis. The $HAuCl_4$ oxidizes the C=C double bond to cause the formation of an aldehyde group or a hydroxyl group on one side and a carboxyl group on the other (*i.e.*, CHO-R-COOH or HO-R-COOH), allowing the location of the double bond to be identified. This approach was successfully applied to four unsaturated fatty acids [linoleic acid (LA), ricinoleic acid (RA), isooleic acid (IA), and nervonic acid (NA)] and two phospholipids [1,2-dioleoyl-*sn*-glycero-3-phosphocholine (DOPC) and L-α-lysophosphatidylcholine (lysoPC)]. A mechanism for this transformation is proposed, which involves epoxidation of the double bond, followed by the formation of the final products. This method has the advantages of being simple and rapid, and requiring a small amount of analyte.

Introduction

In modern lipidomic analysis, mass spectrometry (MS) has become the method of choice because of its sensitivity, its ability to achieve spatial imaging, and its simultaneous recording of numerous different lipids, fatty acids, and metabolites.[1] MS is based on measuring the mass-to-charge ratios of different species. Consequently, it is unable to discern structural differences that cause no mass change, such as the location of carbon–carbon double bonds in a long hydrocarbon chain. Accordingly, numerous degradation and derivatization steps are required to achieve a comprehensive structural analysis of lipids. This challenge, which is often very time consuming, becomes even more severe in mass spectrometry imaging (MSI) because the lipid amount is much reduced.

One popular and successful approach is ozone-induced dissociation.[2–17] In this approach, it is typical to mass-select the lipid ion and expose it to ozone vapor, followed by collision-induced dissociation (CID), which allows the position of the double bond to be assigned unambiguously from the fragmentation data. Other online double-bond derivatization methods prior to mass spectrometric analysis have also been employed,[18–23] in particular, the tagging of the C=C bond with acetone *via* the photochemical Paternó–Büchi reaction, followed by CID of the tagged ionic species.[24–26] Much success has already been achieved in the structural analysis of lipids, but these approaches require extra instrumentation for derivatization and for carrying out tandem mass spectrometry. These facts motivate a search for a possibly simpler method for determining the location of double bonds. Recently, Tang, Cheng, and Yan[27] have introduced a new derivatization approach in which electrochemical epoxidation is introduced into unsaturated structures by means of standard nano-electrospray mass spectrometry. On-demand formation of one or more epoxides is achieved at different voltages. The electro-epoxidized products are then fragmented by tandem MS to generate diagnostic ions, indicating the double bond position(s). Thus, the derivatization step is avoided. In a similar spirit, we have avoided the use of tandem MS by adding an oxidizing agent into an electrospray solvent so that the resulting oxidation products, as recorded by a mass spectrometer, can be used to identify the location of one or more carbon–carbon double bonds in the analyte of interest.

Our approach takes advantage of several unique aspects of microdroplet chemistry. It has become established that the rates of chemical reactions in microdroplets can be accelerated by factors of a thousand or more compared to the same reactions in bulk solvent.[28] Moreover, microdroplet reactions can yield new reaction products, a striking example being the formation of gold nanoparticles and nanowires when aqueous microdroplets containing chloroauric acid ($HAuCl_4$) are

[a]*Department of Chemistry, Fudan University, Jiangwan Campus, Shanghai 200438, China. E-mail: rnz@fudan.edu.cn*
[b]*Department of Chemistry and Environmental Science, New Jersey Institute of Technology, Newark, NJ 07102, USA*

†Electronic supplementary information (ESI) available. See DOI: 10.1039/d0an02396e

sprayed at room temperature in the air onto some surface, such as a glass microscope slide.[29] When histidine (His) is mixed with $HAuCl_4$ and sprayed, it has been reported that the active catalytic species $[Au + 2His - 2H]^-$ is directly formed.[30] Clear evidence has been presented that tiny water droplets contain reactive oxygen species (ROS), such as the hydroxyl radical (OH), which leads to the formation of hydrogen peroxide (HOOH).[31–34] In this study we take advantage of the oxidizing power of 10 μM chloroauric acid in water microdroplets by applying it to four unsaturated fatty acids [linoleic acid (LA), ricinoleic acid (RA), isooleic acid (IA), and nervonic acid (NA)] and two phospholipids [1,2-dioleoyl-*sn-glycero*-3-phosphocholine (DOPC) and L-α-lysophosphatidylcholine (lysoPC)] for the purpose of identifying the locations of C=C double bonds in these unsaturated organic compounds by means of microdroplet mass spectrometry.

Materials and methods

Chemicals

Gold(III) tetrachloride trihydrate ($HAuCl_4 \cdot 3H_2O$), linoleic acid (LA), ricinoleic acid (RA), isooleic acid (IA), and nervonic acid (NA) were purchased from Sigma-Aldrich (St Louis, MO). 1,2-Dioleoyl-*sn-glycero*-3-phosphocholine (DOPC) and L-α-lysophosphatidylcholine (lysoPC) were purchased from AVT (Shanghai) Pharmaceutical Tech Co., Ltd. All these compounds were used without further purification. Sodium hydroxide (NaOH), hydrochloric acid (HCl), hydrogen peroxide (H_2O_2, 30%), and ethanol were purchased from Adamas (Tansoole, China). Water was purified using a Milli-Q system (Millipore, Bedford, MA, USA) with a resistivity of 18.2 MΩ cm and used throughout.

Analysis by QTOF MS

The sample solution was sprayed from the tip of a piece of fused silica capillary (148 μm o.d., 50 μm i.d., Polymicro Technologies, China) of a homemade sprayer, which is assisted by a nebulizing gas of dry N_2 with a pressure of 60 psi (Fig. 1a). The sample solution containing unsaturated fatty acids (100 μM) or lipids (50 μg mL^{-1}) and chloroauric acid ($HAuCl_4$, 10 μM) was ejected from the nanocapillary using a micropump (KD Scientific) with a 1 mL syringe (Hamilton), which was connected by a piece of fused silica capillary between the needle and the nanocapillary emitter. Different high voltage polarities were applied on the needle to form microdroplets at the tip of the homemade spray source. The sample injection flow rate was precisely set to 5 μL min^{-1} using the micropump. By setting a flight distance of 10 mm between the tip of the sprayer and the inlet of a high-resolution Q-TOF mass spectrometer (Synapt G^2, Waters, USA), the MS spectrum was recorded in the mass range of 100–1000 Da. The MS inlet capillary was always maintained at 150 °C and the capillary voltage at 0 V. No other nebulizing gases were used when performing microdroplet reactions.

Results and discussion

Microdroplet mass spectrum of chloroauric acid ($HAuCl_4$)

Fig. 2a presents the mass spectrum when a 10 μM $HAuCl_4$ aqueous solution was sprayed at −4.5 kV using a spray source shown in Fig. 1. In this mass spectrum, the peaks with *m*/*z* values of 266.9054, 498.8345, and 568.7991 correspond to the reduced species of $AuCl_2^-$ (oxidation number + 1), $Au_2Cl_3^-$ (oxidation number + 1) and $Au_2Cl_5^-$ (oxidation number + 2), respectively. We did not observe the obvious peak of the original anion $AuCl_4^-$ (oxidation number + 3); instead, the peak of $AuCl_2^-$ appeared with the highest intensity. This result showed that $HAuCl_4$ could be reduced at a flight distance of 10 mm from the tip of the homemade spray source to the heated inlet of the mass spectrometer. As mentioned in the Methods section, the concentration of $HAuCl_4$ and the pressure of sheath gas (N_2) were optimized to 10 μM and 60 psi, respectively, to produce the highest yield of $AuCl_2^-$ (Fig. 2b and c).

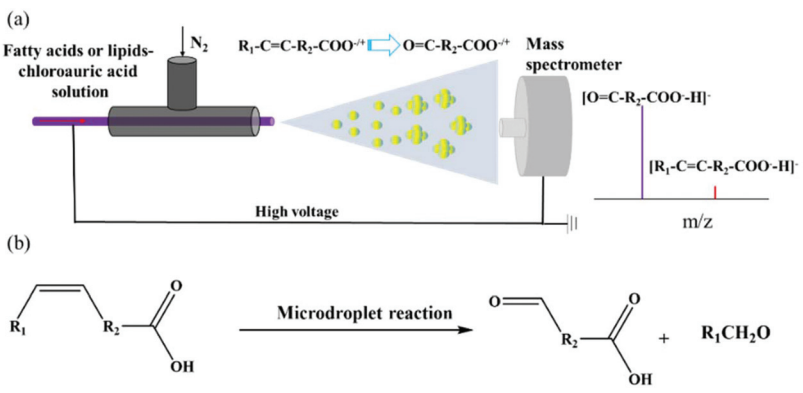

Fig. 1 (a) Schematic of the experimental apparatus for the online microdroplet reaction coupled with a mass spectrometer (microdroplet-MS) with a N_2 gas pressure of 60 psi. (b) Schematic of the microdroplet reaction with unsaturated fatty acids (100 μM) or lipids (50 μg mL^{-1}) and chloroauric acid ($HAuCl_4$, 10 μM) at high voltages (−4.5 kV for the negative ion mode and +4.0 kV for the positive ion mode). The travel distance of the microdroplets from the spray source to the heated inlet (150 °C) of the mass spectrometer is 10 mm.

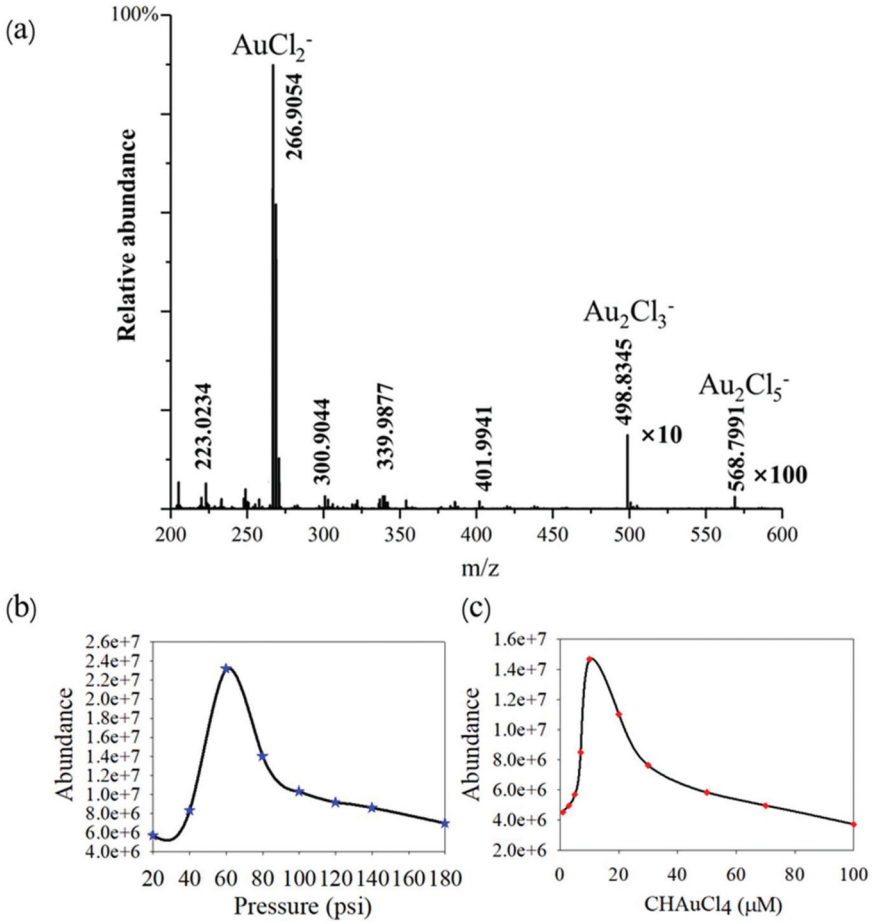

Fig. 2 Microdroplet mass spectrometry of $HAuCl_4$ (10 μM): (a) mass spectrum; (b) $AuCl_2^-$ intensity as a function of different pressures of N_2 sheath gas; (c) $AuCl_2^-$ intensity as a function of different concentrations of $HAuCl_4$.

Unsaturated fatty acid analysis *via* a $HAuCl_4$ microdroplet reaction

Isooleic acid (IA, (18 : 1(11Z)) is a monounsaturated fatty acid, where the C=C bond is located between C_{11} and C_{12}. As a control experiment, IA (100 μM) was dissolved in a mixture of ethanol and water (2/98, v/v), and sprayed into the mass spectrometer under the above-described conditions in the negative ion mode. The resulting mass spectrum (Fig. 3a) showed only three species with *m*/*z* values of 281.2, 297.2, and 313.2, which correspond to $[IA - H]^-$, $[IA + O - H]^-$, and $[IA + 2O - H]^-$, respectively. Compared to the abundance of $[IA - H]^-$, only a small amount of $[IA + O - H]^-$ and $[IA + 2O - H]^-$ was formed, presumably from the presence of ROS species in the water microdroplets. When 10 μM $HAuCl_4$ is added to the dissolved IA, new species with *m*/*z* values of 199.1 and 297.2 appear with relative abundances of 64% and 15% of the IA signal in the mass spectrum with a flight distance of 10 mm, respectively (Fig. 3b). An increase of the flight distance from 15 mm to 40 mm causes some new species to appear in the mass spectrum (Fig. S1, S2, and S3†). By reference to the previously studied photochemical Paternó–Büchi reaction of IA,[26] the species with an *m*/*z* value of 199.1 matches closely with a similar result of IA (18 : 1(11Z)) for the diagnostic ion in the CID mode of tandem mass spectrometry. The results further revealed that this species has carboxyl and aldehyde groups with the formula $[C_{11}H_{20}O_3 - H]^-$ in the negative ion mode, which means that the C=C bond in IA (18 : 1(11Z)) has been

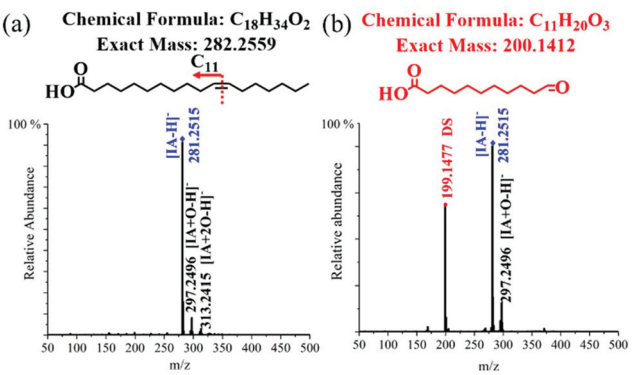

Fig. 3 Elucidation of the location of C=C in IA (18 : 1(11Z)). Mass spectra of (a) IA and (b) IA + $HAuCl_4$ obtained using a microdroplet mass spectrometer with a flight distance of 10 mm.

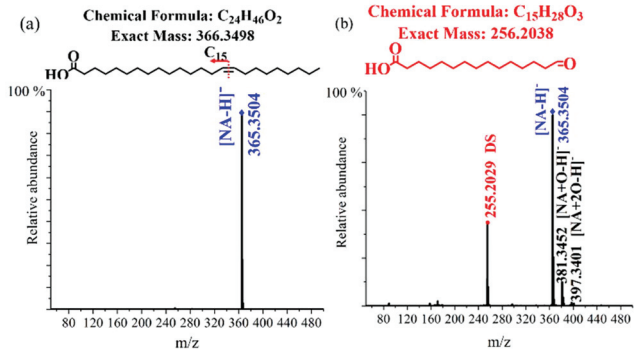

Fig. 4 Elucidation of the location of C=C in NA (24 : 1(15Z)). Mass spectra of (a) NA and (b) NA + $HAuCl_4$ obtained using a microdroplet mass spectrometer with a flight distance of 10 mm.

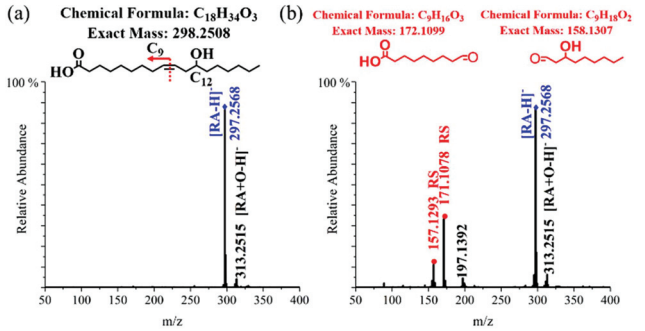

Fig. 5 Elucidation of the location of C=C in RA (18 : 1(9Z)). Mass spectra of (a) RA and (b) RA + $HAuCl_4$ obtained using a microdroplet mass spectrometer with a flight distance of 10 mm.

broken between C_{11} and C_{12} in the $HAuCl_4$–IA microdroplet reaction.

Similarly, nervonic acid (NA, (24 : 1(15Z)) is a monounsaturated fatty acid with a chain length of 24 carbon atoms and a C=C bond located between C_{15} and C_{16}. As a control experiment, NA (100 μM) was dissolved in a mixture of ethanol and water (2/98, v/v), and sprayed into the mass spectrometer under the above-described conditions in the negative ion mode. The resulting mass spectrum (Fig. 4a) showed only one species with an *m/z* value of 365.4, which corresponds to $[NA - H]^-$. Compared with the peaks of $[IA + O - H]^-$ and $[IA + 2O - H]^-$ found in the mass spectrum of IA, the only peak of $[NA - H]^-$ found in the mass spectrum may be attributed to the different long carbon chain and C=C location between IA (18 : 1(11Z)) and NA (24 : 1(15Z)). It will affect the attack ability of the hydrophilic free radicals for the C=C bond at the air–water interface of the microdroplets. When 10 μM $HAuCl_4$ is added to the dissolved NA, new species with *m/z* values of 381.3 $[NA + O - H]^-$, 397.3$[NA + 2O - H]^-$, and 255.2 appear with relative abundances of 8%, 2% and 34% of the NA signal in the mass spectrum with a flight distance of 10 mm, respectively (Fig. 4b), while at a flight distance of 20 mm, some new species were found as intermediate species (Fig. S4, S5, and S6†). Similarly, the species with an *m/z* value of 255.2 is a diagnostic ion of NA (24 : 1(15Z)) for pinpointing the location of the fatty acid C=C bond.

For the monounsaturated fatty acid ricinoleic acid (RA, 18 : 1(9Z)) with a chain length of 18 carbon atoms and the C=C bond located between C_9 and C_{10}, there is one hydroxyl substituent group on the position of C_{12}. As a control experiment, only two species with *m/z* values of 297.3 $[RA - H]^-$ and 313.2 $[RA + O - H]^-$ were found in the mass spectrum (Fig. 5a). When 10 μM $HAuCl_4$ was added, some new species with *m/z* values of 157.1, 171.1, and 197.1 were found in the mass spectrum with a flight distance of 10 mm (Fig. 5b). With reference to the above microdroplet reaction study for IA and NA, the species of 157.1 and 171.1 are the diagnostic ions for the location of C=C between C_9 and C_{10}, as expected. The species at 171.1 is a diagnostic ion with a carboxyl group. However, the species at 157.1 is a new diagnostic species, which connects with the other part of the RA fragment with the aldehyde group of C_{10} and the hydroxyl group of C_{12}. The reason for this lies perhaps in the hydroxyl group at C_{12} that could improve the ionization efficiency in the negative ion mode, which is different from the others (*e.g.*, OA, IA, and LA mentioned later) with only aldehyde group fragment species.

The linoleic acid (LA, 18 : 2(9Z, 12Z)) with a chain length of 18 carbon atoms has two C=C bonds located between C_9 and C_{10} and between C_{12} and C_{13}. For the LA (18 : 2(9Z, 12Z)), two species with *m/z* values of 279.2 $[LA - H]^-$ and 295.2 $[LA + O - H]^-$ were found in the mass spectrum (Fig. 6a). When 10 μM $HAuCl_4$ was added, some new species with *m/z* values of 225.1, 211.1, and 171.1 were found in the mass spectrum (Fig. 6b). With reference to the previous study of RA, the species of 171.1 matches well with the diagnostic ion for RA. The species of 211.1 is a new species with one C=C at the locations of C_9 and C_{10}, which is caused by the cleavage of the second C=C bond at the locations of C_{12} and C_{13}. The peak with an *m/z* value of 225.1 would be the intermediate for the formation of C_9 and C_{10}, which is obtained by further epoxidation of the C=C bond by the ROS at the air–water interface in the microdroplet reaction. Fig. 6c shows the possible mechanism for the two-diagnostic species of 171.1 and 211.1, which is reported by the Ma group by the epoxidation method,[23] and the one intermediate species of 225.1 for the reaction of LA with $HAuCl_4$ in microdroplet mass spectrometry.

Based on the above results obtained for identifying the location of C=C in the unsaturated fatty acids in microdroplet mass spectrometry, especially with $HAuCl_4$ as the oxidizing agent, some conclusions are as follows:

(1) There exist some oxidized species in the unsaturated fatty acids in the microdroplet mass spectrometry with the formation of $[R + O - H]^-$ and $[R + 2O - H]^-$, which may come from the oxidation caused by the ROS, especially the hydroxyl radical OH, at the water–air interface of the microdroplets, which have been confirmed by the spontaneous generation of H_2O_2 from aqueous microdroplets.[31–33] When $HAuCl_4$ is added as an oxidizing agent, some new special species are

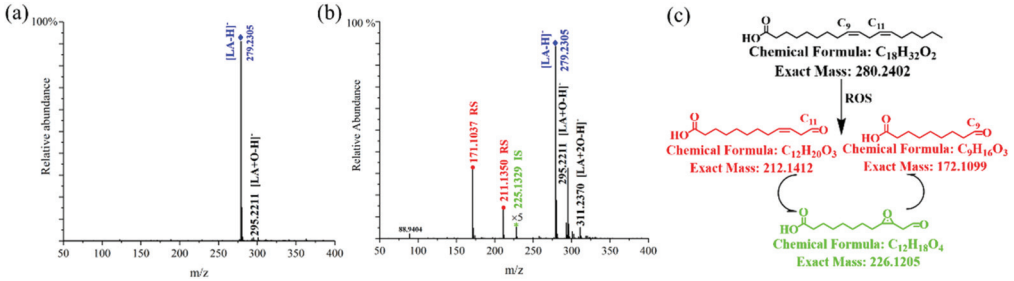

Fig. 6 Elucidation of the location of the C=C bond in LA (18 : 2(9Z, 12Z)). Mass spectrum of (a) LA and (b) LA + $HAuCl_4$ using a microdroplet mass spectrometer with a flight distance of 10 mm. (c) The possible formation mechanism of the two diagnostic ion species and intermediate species of LA with $HAuCl_4$ as the oxidizing agent using a microdroplet mass spectrometer.

found in the mass spectrum. In all these special species, some are diagnostic ions for identifying the location of the C=C bond in the corresponding unsaturated fatty acids, and other species are intermediates which are produced by the ROS reaction. These results revealed that $HAuCl_4$ as the oxidizing agent could effectively promote the abundant ROS formation and accumulation at the air–water interface of the microdroplets. We propose a possible reaction for reducing $AuCl_4^-$ to Au at the air–water interface of the microdroplets with the ROS

$$2AuCl_4^- + 6H_2O + 6OH^\bullet \rightarrow 2Au + 6H_2O_2 + 6H^+ + 8Cl^- \quad (1)$$

which has the lowest Gibbs free energy compared to the bulk reaction system.[35] Corresponding to this equation, the abundant H_2O_2 or potential ROS produced at the air–water interface of the microdroplets would promote oxidation and breakage of the C=C bond in unsaturated fatty acids to form diagnostic ions in the mass spectrum. As a control experiment, unsaturated fatty acids are directly added to an aqueous solution containing $HAuCl_4$–H_2O_2 solution. To eliminate possible false positive results in the microdroplet mass spectrum, ^1H NMR was employed to check the changes. The results showed that there were no obvious changes.

(2) In microdroplet mass spectrometry using $HAuCl_4$ as the oxidizing agent for unsaturated fatty acids, the results revealed that two species would be formed with an aldehyde group at the two sides of the location of the C=C bond (COOH-R_1-CHO and R_2-CHO), which is supported by C=C oxidation by ozone or other ROS reported in the previous literature.[26] It has been shown that the aldehyde products are the ultimate products of epoxidation for the breakage of the C=C bond of unsaturated fatty acids. Note that only the species with the carboxyl group (COOH-R_1-CHO) could be found by the full MS scan due to its good ionization ability. The species with aldehyde (R_2-CHO) as the neutral group could not be detected owing to its weak ionization ability. Through this strategy, the species with the carboxyl and aldehyde groups (COOH-R_1-CHO) in the full-scan mass spectrum could simply and easily be used as diagnostic species for identifying the locations of C=C bonds in unsaturated fatty acids. If a special polar group (like –OH) is contained in the R_2-CHO product, the polar group will affect the ionization efficiency of R_2-CHO and serve as a second diagnostic species (HO-R_n-CHO) in the full-scan mass spectrum.

The mechanism of the microdroplet reaction induced by using $HAuCl_4$ as the oxidizing agent is not definitely determined. Nevertheless, this method has several obvious advantages in identifying the location of C=C bonds in unsaturated fatty acids. We further illustrate the power of this strategy by applying it to a few lipids.

Lipids analysis *via* microdroplet mass spectrometry

The lipid 1-oleoyl-2-hydroxy-*sn*-glycerol-3-choline phosphate (lysoPC, 18 : 1(9Z)) was selected for the study. LysoPC (50 μg mL^{-1}) was dissolved in a solution of ethanol and water (2/98, v/v), and sprayed into the mass spectrometer under the above-described conditions. To obtain a good intensity, NaOH and HCl were added to adjust the pH value from 2.0 to 10.0 of the lysoPC solution, and to investigate the dependence on pH. This allowed us to improve the oxidative efficiency of the microdroplet reaction.

We found good intensity and specificity for the identification of the double bond in lysoPC by means of microdroplet mass spectrometry over the pH range of 2.0–10.0, but with different fragment species. We suggested that different fragment species in the mass spectrum arise from different degradation mechanisms during the time when microdroplet travels from the ESSI source to the inlet of the mass spectrometer. For a pH value of 4.0, there are primarily three species with *m*/*z* values of 522.4 $[M]^+$, 339.3 $[R_1P_1 + H]^+$, and 184.1 $[R_1P_2]^+$ in the mass spectrum (Fig. 7a). The above results showed that lysoPC may have undergone hydrolysis in the acid environment of the microdroplet reaction, and formed the head group with phosphorylcholine (R_1P_2) and the oleoylglycerol ester (R_1P_1).[18] For a pH value of 8.0, we observe different species with *m*/*z* values of 544.3 $[M + Na]^+$, 486.3 $[R_2P_1 + Na]^+$, and 339.3$[R_1P_1 + H]^+$ in the mass spectrum (Fig. 7b). It was observed that lysoPC easily undergoes choline loss accompanied by a hydrolysis reaction in the alkaline environment of the microdroplet.[36]

According to previous reports about the microdroplet characterization of the alkaline or salt environment of the outer layer of a microdroplet,[37] especially the hydroxyl anion distribution at the air–water interface plays the main role in

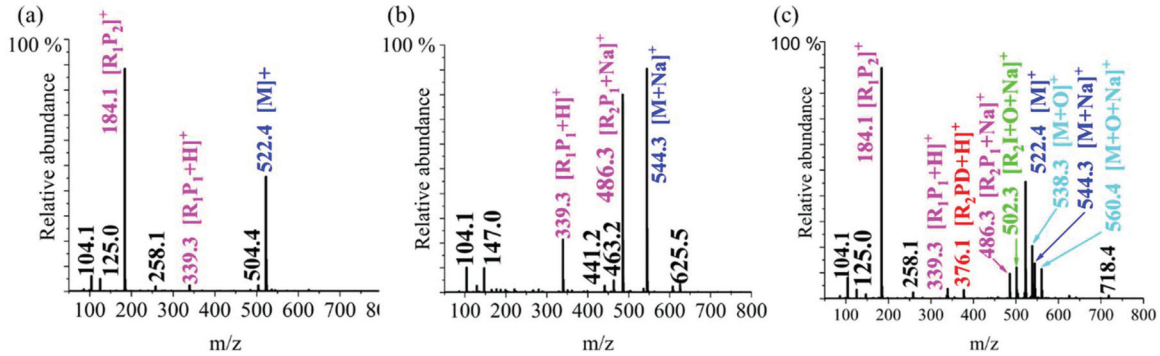

Fig. 7 Elucidation of the location of C=C in lysoPC (18 : 1(9Z)). Mass spectra of lysoPC for (a) acidic (pH = 4) and (b) basic (pH = 8) conditions. (c) The mass spectrum of lysoPC + $HAuCl_4$ (pH = 8) using a microdroplet mass spectrometer.

choline loss in lysoPC which goes on to promote the special chemical reaction for the microdroplet reaction. In view of this, pH = 8.0 was set as the condition for the lysoPC + $HAuCl_4$ microdroplet reaction, which is similar to the condition of physiological pH of lipids. When 10 μM $HAuCl_4$ was added, new species with *m*/*z* values of 376.1, 502.3, 538.3, and 560.4 were found, which correspond to the fragments $[R_2P_1R + Na]^+$, $[R_2P_1I + O + Na]^+$, $[M + O]^+$, and $[M + O + Na]^+$, respectively, in the mass spectrum with a mass error less than 4.1 ppm (Fig. 7c). The species at 502.3 corresponds to the addition of one oxygen atom to the intermediate of $[R_2P_1 + O + Na]^+$, which suggests the formation of the mono-epoxidized product of lysoPC after choline loss in the $HAuCl_4$ + lysoPC microdroplet reaction.[38] Meanwhile, compared with the result of lysoPC in microdroplet mass spectrometry, we observe significant oxidation species of $[M + O]^+$and $[M + O + Na]^+$ by the ROS in the microdroplets after $HAuCl_4$ addition. The presence of a diagnostic ion with an *m*/*z* of 376.1 suggests that the C=C bond is located between C_9 and C_{10} in the structure of lysoPC.

According to these species found in the lysoPC microdroplet mass spectrometry with $HAuCl_4$ as the oxidizing agent, the possible mechanisms for lysoPC fragmentation are presented in Fig. 8 under the pH conditions of 4.0 and 8.0. At a pH of 4.0, lysoPC mainly underwent a hydrolysis reaction and formed the fragment of the oleoylglycerol ester $[R_1P_1 + H]^+$ and the head group of phosphorylcholine $[R_1P_2]^+$ with *m*/*z* values of 339.3 and 184.1, respectively. Unfortunately, further oxidation fragment species for $[R_1P_1 + H]^+$ and $[R_1P_2]^+$ were not found when $HAuCl_4$ was added. The reason might be that they have little or no reactive oxidative species (ROS) promoted by the $HAuCl_4$ under acidic conditions. In contrast to the acidic conditions, different fragmentation paths for lysoPC appear under alkaline conditions when $HAuCl_4$ is added.

We summarize these results as follows: (1) the alkaline condition will mediate the de-choline reaction of lysoPC with the formation of choline $[R_2P_2]^+$ and diacylglycerophosphate $[R_2P_1 + Na]^+$ species in the mass spectrum; (2) $HAuCl_4$ as the oxidizing agent will promote the epoxidation of C=C of $[R_2P_1 + Na]^+$ to form the intermediate ion of $[R_2P_1 + O + Na]^+$, which is the intermediate species for the epoxidation of C=C; (3) the intermediate species of $[R_2P_1 + O + Na]^+$ was opened by causing the epoxidation of the C=C bond to form the aldehyde group at the end position of C_9 and C_{10} to form the diagnostic ion $[R_2P_1D + Na]^+$.

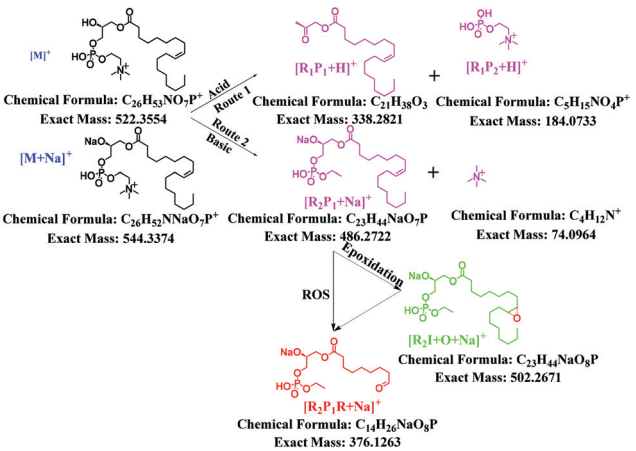

Fig. 8 Possible mechanism for the different species formed in the lysoPC + $HAuCl_4$ microdroplet reaction under both acidic and basic conditions.

We also examined dierucoyl phosphatidylcholine (DOPC, 18 : 2(11Z,11Z)) as a lipid, having two C=C bonds. Here, 50 μg mL^{-1} DOPC water solution was prepared by dissolving this compound in an ethanol and water (2/98, v/v) mixture with pH values of 4.0 and 8.0. The solution was sprayed into a mass spectrometer under the above-described conditions in the positive ion mode. For the pH value of 4.0, species with *m*/*z* values of 786.6, 802.6, and 818.6 were found in the mass spectrum which correspond well to $[DOPC]^+$, $[DOPC + O]^+$, and $[DOPC + 2O]^+$, respectively. We also observed a species at an *m*/*z* value of 184.1, which corresponds to DOPC undergoing hydrolysis and losing phosphorylcholine, which is the head group. The species at 802.6 and 818.6 correspond to the addition of one oxygen atom and two oxygen atoms to the molecule of DOPC, respectively (Fig. 9a). At pH = 8.0, in addition to the species at 184.1 already identified, species with *m*/*z* values of 786.7 and 808.6 were found, which correspond to

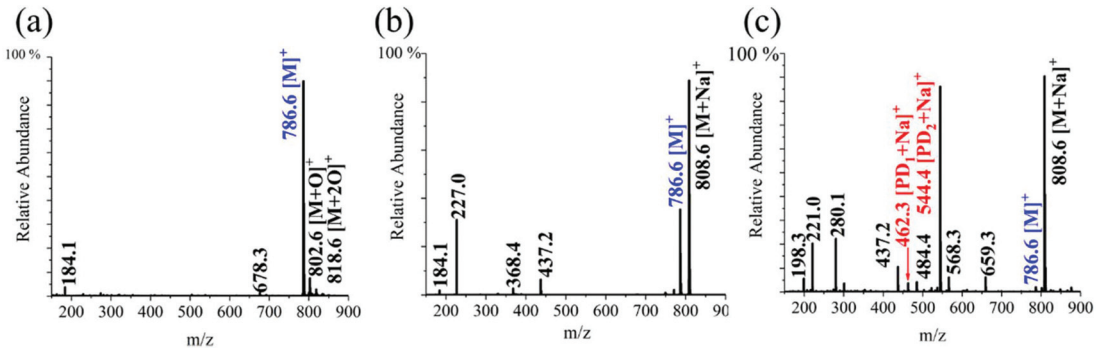

Fig. 9 Elucidation of the location of the C=C bond in DOPC (18 : 2(11Z, 11Z)). Mass spectrum of DOPC for (a) acidic and (b) basic conditions in the microdroplet reaction. (c) Mass spectrum of DOPC + $HAuCl_4$ under basic conditions in the microdroplet reaction.

the fragment of $[DOPC]^+$ and $[DOPC + Na]^+$, respectively. There was hardly any choline loss for DOPC in the alkaline microdroplet, only with the characteristic ion peak with sodium addition (Fig. 9b). When 10 μM $HAuCl_4$ is added, we observe new species with *m/z* values of 544.4 and 462.3, which correspond to the diagnostic species $[PD_1]^+$ (*m/z* 522.4284) and $[PD_2]^+$ (*m/z* 440.3138) with mass errors less than 3.9 ppm when removing the sodium ion in the species of $[PD_1 + Na]^+$ and $[PD_2 + Na]^+$, respectively (Fig. 9c). Unfortunately, no intermediate species of epoxidation of DOPC was found in this $HAuCl_4$ + DOPC microdroplet reaction. Similar results for DOPC (18 : 1 (9)–18 : 1(9)) were reported by Yan and coworkers[27] by electrochemical epoxidation accompanied by tandem mass spectrometry in the CID mode. Interestingly, the $[PD_1 + Na]^+$ and $[PD_2 + Na]^+$ species have abundances of 10% and 90% relative to the sodium ion of the DOPC signal, which reveals that the location of two C=C bonds in DOPC could be detected at the same time.

The different abundances of the species of $[PD_1 + Na]^+$ obtained in the full scan mass spectrum may be attributed to the different accumulation effects of microdroplet reactions for the two single C=C chains in DOPC. For $[PD_2 + Na]^+$, this means that the C=C bonds of the two chains in DOPC were simultaneously oxidized by the ROS produced in the microdroplet reaction. By combining the information of $[PD_1 + Na]^+$ and $[PD_2 + Na]^+$ species, we are led to propose the mechanism for the DOPC + $HAuCl_4$ microdroplet reaction given in Fig. 10.

From the mass spectrum result of lysoPC and DOPC obtained by microdroplet mass spectrometry, we have demonstrated the feasibility of using lipid + $HAuCl_4$ microdroplet reactions for determining the location of C=C double bonds in lipids. A summary follows:

(1) Phosphatidylcholine (PC) type lipids have different degradation mechanisms in acidic or basic microdroplet reactions. Obviously, it is easy to lose phosphatidylcholine (PC, head group of lipids) and form the species of diacylglycerol in acidic microdroplet mass spectrometry. However, in the basic environment, microdroplets have the ability to cause choline loss from the PC group. This behavior cannot be explained by in-source fragmentation from the heated inlet of the mass

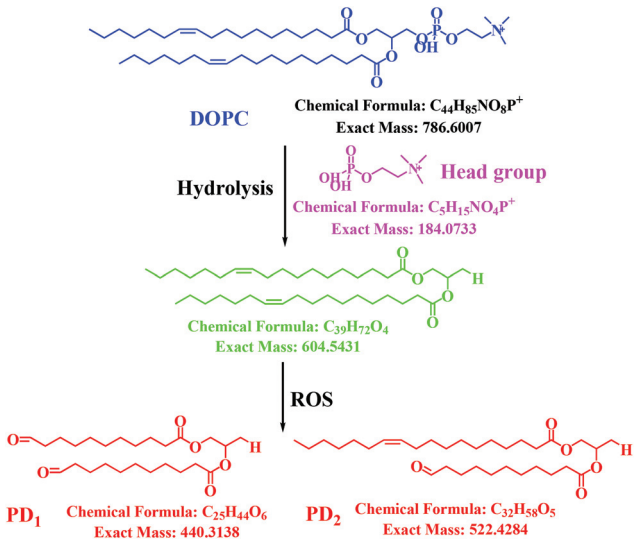

Fig. 10 Possible mechanism for the formation of different species in the DOPC + $HAuCl_4$ microdroplet reaction under basic conditions.

spectrometer[39] and the different acid or alkaline mediated microdroplet reaction cannot be attributed to evaporation of the aqueous microdroplet during the time of flight from the spray source to the mass spectrometer.[40]

(2) The addition of $HAuCl_4$ to the spray solution promotes the potential oxidation of the lipid in the microdroplet. Possible mechanisms for lysoPC and DOPC have been proposed. As a control experiment, when10 μ M H_2O_2 solution is added to the $HAuCl_4$, no reduced species of $AuCl_2^-$ (oxidation number + 1), $Au_2Cl_3^-$ (oxidation number + 1) or $Au_2Cl_5^-$ (oxidation number + 2) were observed in the mass spectrum. Instead, the transparent aqueous solution of $AuCl_4^-$ with H_2O_2 gradually changes to apricot, which reveals the formation of gold nanoparticles in this bulk reaction. We propose a possible reaction for $AuCl_4^-$ reduction in H_2O_2 under acidic or basic conditions:[35]

$$2AuCl_4^- + 3H_2O_2 \rightarrow 2Au + 3O_2 + 6H^+ + 8Cl^- \quad (2)$$

$$2AuCl_4^- + 3H_2O_2 + 6OH^- \rightarrow 2Au + 6H_2O + 3O_2 + 8Cl^- \quad (3)$$

Both reactions are accompanied by the generation of O_2 in the formation of Au nanoparticles. After adding lysoPC and DOPC, there were no species of diagnostic ions found in the full-scan mass spectrum. This result confirms that it is the special environment of the microdroplet that produced ROS species at the microdroplet interface, which promotes oxidation of C=C double bonds in lipids.

(3) Compared with the reported methods of epoxidation of C=C in DOPC by electrochemical oxidation[28] or by the Paternó–Büchi reaction[25] for lysoPC structural analysis by mass spectrometry, the method we have presented directly provides information for the location of one or more C=C double bonds without the use of tandem mass spectrometry.

Conclusions

We have shown that the addition of $HAuCl_4$ to an aqueous spray solution containing organic molecules with one or more C=C double bonds leads to diagnostic ions being produced when forming microdroplets that travel a short distance to a mass spectrometer for chemical analysis. The masses of these diagnostic ions allow the position of the double bonds in the parent molecule to be determined unambiguously. To illustrate the power of this method, we have applied it for determining the C=C bond location of four different unsaturated fatty acids and two different lipids using a homemade ESSI source and a commercial mass spectrometer. We speculate that microdroplet reactions using $HAuCl_4$ as an oxidizing agent might lead to the formation and accumulation of many different reactive oxygen species (ROS) at the air–water interface of the microdroplets which then attack the C=C double bond to form characteristic diagnostic ions. More work is needed to elucidate the details of this process.

It is important to stress that this is the first study of this method and represents primarily a proof of principle. There are missing aspects of this study that need to be addressed in the future. One of them is to determine the limits of detection, although the present study shows good promise of being sufficiently sensitive for many purposes. Another limitation is that the present study has not analyzed a complex mixture of lipids for which it might be necessary to make several runs with different concentrations of $HAuCl_4$ to distinguish between patents and fragments. Nevertheless, the method presented here does show promise in aiding the analyst in carrying out the structural analysis of organic molecules containing one or more C=C double bonds.

Author contributions

K. L., H. C., and R. N. Z. wrote this manuscript together and discussed the results and their interpretation. All experimental data were taken by K. L.

Conflicts of interest

All authors declare no conflict of interest.

Acknowledgements

This work was supported by the Scientific Research Startup Foundation (Grant No.: IDH1615113) of Fudan University and the National Natural Science Foundation of China (Grant No.: 22072122 and 21974027).

References

1 S. J. Blanksby and T. W. Mitchell, *Annu. Rev. Anal. Chem.*, 2010, **3**, 433–465.
2 M. C. Thomas, T. W. Mitchell and S. J. Blanksby, *J. Am. Chem. Soc.*, 2006, **128**, 58–59.
3 M. C. Thomas, T. W. Mitchell, J. M. Deeley, D. G. Harman, R. C. Murphy and S. J. Blanksby, *Anal. Chem.*, 2007, **79**, 5013–5022.
4 M. C. Thomas, T. W. Mitchell, D. G. Harman, J. M. Deeley, J. R. Nealon and S. J. Blanksby, *Anal. Chem.*, 2008, **80**, 303–311.
5 S. H. J. Brown, T. W. Mitchell and S. J. Blanksby, *Biochim. Biophys. Acta*, 2011, **1811**, 807–817.
6 H. T. Pham, A. T. Maccarone, J. L. Campbell, T. W. Mitchell and S. J. Blanksby, *J. Am. Soc. Mass Spectrom.*, 2013, **24**, 286–296.
7 H. T. Pham, A. T. Maccarone, M. C. Thomas, J. L. Campbell, T. W. Mitchell and S. J. Blanksby, *Analyst*, 2014, **139**, 204–214.
8 M. R. L. Paine, B. L. J. Poad, G. B. Eijkel, D. L. Marshall, S. J. Blanksby, R. M. A. Heeren and S. R. Ellis, *Angew. Chem., Int. Ed.*, 2018, **57**, 10530–10534.
9 N. Vu, J. Brown, K. Giles and Q. Zhang, *Rapid Commun. Mass Spectrom.*, 2017, **31**, 1415–1423.
10 B. L. J. Poad, M. R. Green, J. M. Kirk, N. Tomczyk, T. W. Mitchell and S. J. Blanksby, *Anal. Chem.*, 2017, **89**, 4223–4229.
11 R. A. Harris, J. C. May, C. A. Stinson, Y. Xia and J. A. McLean, *Anal. Chem.*, 2018, **90**, 1915–1924.
12 B. L. J. Poad, X. Zheng, T. W. Mitchell, R. D. Smith, E. S. Baker and S. J. Blanksby, *Anal. Chem.*, 2018, **90**, 1292–1300.
13 R. C. Barrientos and Q. Zhang, *J. Am. Soc. Mass Spectrom.*, 2019, **30**, 1609–1620.
14 B. L. J. Poad, D. L. Marshall, E. Harazim, R. Gupta, V. R. Narreddula, R. S. E. Young, E. Duchoslav, J. L. Campbell, J. A. Broadbent, J. Cvačka, T. W. Mitchell and S. J. Blanksby, *J. Am. Soc. Mass Spectrom.*, 2019, **30**, 2135–2143.
15 R. L. Kozlowski, J. L. Campbell, T. W. Mitchell and S. J. Blanksby, *Anal. Bioanal. Chem.*, 2015, **407**, 5053–5064.

16 S. L. Knowles, N. Vu, D. A. Todd, H. A. Raja, A. Rokas, Q. Zhang and N. H. Oberlies, *J. Nat. Prod.*, 2019, **82**, 3421–3431.
17 S. W. Maddox, R. H. Fraser Caris, K. L. Baker, A. Burkus-Matesevac, R. Peverati and C. D. Chouinard, *J. Am. Soc. Mass Spectrom.*, 2020, **31**, 411–417.
18 D. E. Minnikin, *Chem. Phys. Lipids*, 1978, **21**, 313–347.
19 B. A. Leonhardt and E. D. DeVilbiss, *J. Chromatogr.*, 1985, **322**, 484–490.
20 Y. Kwon, S. Lee, D.-C. Oh and S. Kim, *Angew. Chem., Int. Ed.*, 2011, **50**, 8275–8278.
21 T. H. Kuo, H. H. Chung, H. Y. Chang, C. W. Lin, M. Y. Wang, T. L. Shen and C. C. Hsu, *Anal. Chem.*, 2019, **91**, 11905–11915.
22 K. Chintalapudi and A. K. Badu-Tawiah, *Chem. Sci.*, 2020, **11**, 9891–9897.
23 Y. Zhao, H. Zhao, X. Zhao, J. Jia, Q. Ma, S. Zhang, X. Zhang, H. Chiba, S.-P. Hui and X. Ma, *Anal. Chem.*, 2017, **89**, 10270–10278.
24 X. Ma, X. Zhao, J. Li, W. Zhang, J.-X. Cheng, Z. Ouyang and Y. Xia, *Anal. Chem.*, 2016, **88**, 8931–8935.
25 X. Ma, C. R. Tian, R. Shi, T. Y. Hu, Z. Ouyang and Y. Xia, *Proc. Natl. Acad. Sci. U. S. A.*, 2016, **113**, 2573–2578.
26 R. C. Murphy, T. Okuno, C. A. Johnson and R. M. Barkley, *Anal. Chem.*, 2017, **89**, 8545–8553.
27 S. Tang, H. Cheng and X. Yan, *Angew. Chem.*, 2020, **59**, 209–214.
28 Z. Wei, Y. Li, R. G. Cooks and X. Yan, *Annu. Rev. Phys. Chem.*, 2020, **71**, 31–51.
29 J. K. Lee, D. Samanta, H. G. Nam and R. N. Zare, *Nat. Commun.*, 2018, **9**, 1562.
30 K. Luo, J. Li, Y. Cao, C. Liu, J. Ge, H. Chen and R. N. Zare, *Chem. Sci.*, 2020, **11**, 2558.
31 J. K. Lee, K. L. Walker, H. S. Han, J. Kang, F. B. Prinz, R. M. Waymouth, H. G. Nam and R. N. Zare, *Proc. Natl. Acad. Sci. U. S. A.*, 2019, **116**, 19294–19298.
32 M. T. Dulay, J. K. Lee, A. C. Mody, R. Narasimhan, D. M. Monack and R. N. Zare, *QRB Discovery*, 2020, **1**(e3), 1–8.
33 J. K. Lee, H. S. Han, S. Chaikasetsin, D. P. Marron, R. M. Waymouth, F. B. Prinz and R. N. Zare, *Proc. Natl. Acad. Sci. U. S. A.*, 2020, **117**, 30934–30941.
34 S. Mondal, S. Acharya, R. Biswas, B. Bagchi and R. N. Zare, *J. Chem. Phys.*, 2018, **148**, 244704.
35 Q. Chen, T. Kaneko and R. Hatakeyama, *Appl. Phys. Express*, 2012, **5**, 086201.
36 A. Roux and R. Loewith, *Dev. Cell*, 2017, **6**, 571–572.
37 S. Lhee, J. K. Lee, J. Kang, S. Kato, S. Kim, R. N. Zare and H. G. Nam, *Sci. Adv.*, 2020, **6**, eaba0181.
38 Y. H. Lai, S. Sathyamoorthi, R. M. Bain and R. N. Zare, *J. Am. Soc. Mass Spectrom.*, 2018, **29**, 1036–1043.
39 S. Banerjee and R. N. Zare, *J. Phys. Chem.*, 2019, **123**, 7704–7709.
40 J. K. Lee, H. G. Nam and R. N. Zare, *Q. Rev. Biophys.*, 2017, **50**, 1–7.

